Anomalous Scaling and Structure Instability in Three-Dimensional Passive Scalar Turbulence

Shiyi Chen[1,2] and Nianzheng Cao[1,2]
[1] *IBM Research Division, T. J. Watson Research Center, P.O. Box 218, Yorktown Heights, NY 10598*
[2] *Theoretical Division and Center for Nonlinear Studies, Los Alamos National Laboratory, Los Alamos, NM 87545*

The anomalous scaling phenomena of three-dimensional passive scalar turbulence are studied using high resolution direct numerical simulation. The inertial range scaling exponents of the passive scalar increment and the scalar dissipation are obtained. The connection between the intermittency structure and the scaling exponent is examined and the structure instability of the high amplitude scalar dissipation is used to clarify previous experimental results for the scaling exponents.

PACS numbers: 47.27.-i, 47.27.Gs

The advection of a passive scalar field by a turbulent (or stochastic) incompressible velocity field is a process that exhibits cascade to small scales. The dynamics governing a passive scalar is described by the following equation,

$$\partial T/\partial t + \mathbf{u}\cdot\nabla T = \kappa\nabla^2 T + \mathbf{f}. \qquad (1)$$

Here T is the passive scalar, κ is the kinematic diffusivity, $\mathbf{f}$ is a random forcing, and the advective velocity, $\mathbf{u}$, is governed by the Navier-Stokes (NS) equations in three dimensions.

The study of the dynamics in the passive scalar system has been one of the most active research areas in the field of fluid turbulence for the last decade [1,2]. In particular, based on a linear ansatz for the dissipation term, Kraichnan [2] obtains an explicit prediction of the anomalous scaling exponents for a class of passive scalar advected by a white and Gaussian incompressible velocity. The research has inspired a large number of papers [3] over the past two years, including numerical simulations [4] and analysis of experiments [5].

The passive scalar convected by Navier-Stokes turbulence, however, is a more difficult problem where the velocity is far from white and Gaussian. No inertial range scaling based on the passive scalar dynamical equation (1) has been developed. The local similarity theory for the passive scalar, an extension to Kolmogorov 1941 similarity theory for the velocity field [6], was studied by Obukhov [7] and Corrsin [8]. For fluid flows at very high Reynolds number and with Prandtl number, $Pr = \nu/\kappa$, close to unity, Obukhov's theory assumes the existence of universal statistics of fluctuations at so-called inertial-range scales $L \gg r \gg \eta$, where ν is the kinematic viscosity, L and η are the characteristic length scales for the large scale and the dissipation scale, respectively. This hypothesis has a series of implications, including the 2/3 law for the passive scalar fluctuations in the inertial range: $\langle \Delta T_r^2\rangle \sim \langle\epsilon\rangle^{-1/3}\langle N\rangle r^{2/3}$, where $N = \kappa(\nabla T)^2$ is the scalar dissipation function, ϵ is the velocity dissipation function, $\Delta T_r = T(x+r) - T(x)$ is the scalar increment and $\langle\cdot\rangle$ denotes an ensemble average. In general, if there is a scaling range, the pth order structure function, $S_p(r) = \langle \Delta T_r^p\rangle$, should have a scaling relation: $S_p(r) \sim r^{z_p}$, with z_p defined as the pth order scaling exponent.

Taking account of the intermittency correction [9] and using the refined similarity hypothesis (RSH) [10,11], the phenomenological scaling models for the passive scalar, including the bi-variate log-normal model by Van Atta [12], the β model [13] by Frisch *et. al.* and the bi-variate multifractal model by Meneveau *et. al.* [14], lead to analytical predictions of anomalous scaling exponents. In a recent note, we have developed a bi-variate log-Poisson model [15]; the resulting scaling exponents agree well with experimental measurements.

The challenge in the real-life experimental measurement is to minimize the interference of two probes which measure velocity and scalar quantities simultaneously at the same position [14]. Our research is motivated by the paper by Sreenivasan and Antonia [16] who pointed out that two existing experimental measurements [17,14] do not provide a convergent scaling relation for the passive scalar system. In particular, the scaling exponents in [14] were obtained using the measured dissipation exponents by invoking the RSH, showing a saturation for $p \geq 6$. The scaling exponents from another experimental measurement [18] fall between above two results.

Direct numerical simulation of the passive scalar equation (1) and the Navier-Stokes equations were carried out simultaneously. A mesh size of 512^3 was used in a cyclic cubic box for homogeneous isotropic turbulence. In order to maintain statistical steady states, both the velocity field and the passive scalar field were forced for $k < 3$ [19,20]. The forcing scheme keeps the total energy in the first two shells ($1 \leq k < 2$ and $2 \leq k < 3$) consistent with $k^{-5/3}$. In addition, Fourier modes in each shell have equal energy and the phase of each mode is randomized. For simplicity the Prandtl number is fixed to be unity for this study. The analysis was carried out for the statistical steady states at Taylor microscale Reynolds number $\mathcal{R}_\lambda = 220$. A spatial averaging over the whole physical domain and a time average over approximately 10 large-

eddy turnover time were used to replace the ensemble average.

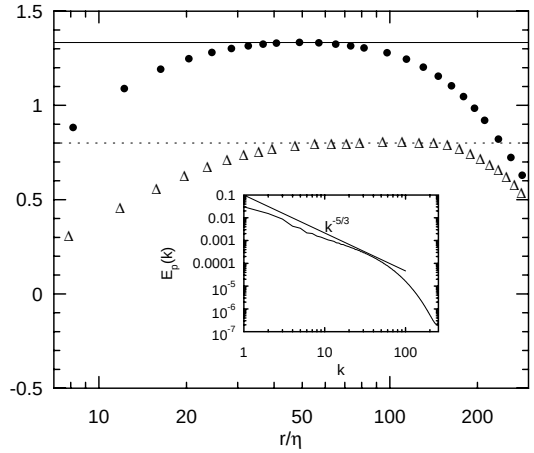

FIG. 1. Numerical verification of Kolmogorov's 4/5 law and Yaglom's 4/3 law. The solid line is for Kolmogorov's 4/5 law and the dashed line is for Yaglom's 4/3 law. The signs are from DNS data ($\triangle$ for $-\langle(\Delta u_r)^3\rangle/(\langle\epsilon\rangle r)$ and $\bullet$ for $-\langle(\Delta u_r(\Delta T_r)^2\rangle/(\langle N\rangle r)$. Here $\eta = (\nu^3/\langle\epsilon\rangle)^{1/4}$ is the Kolmogorov dissipation length, In the inset shows the scalar spectrum compared with Oboukov's $-5/3$ law for the inertial range scaling.

At very high Reynolds number, Kolmogorov's 4/5 law [21] is exact in the inertial range: $\langle(\Delta u_r)^3\rangle = \langle(u(x+r)-u(x))^3\rangle = -4/5\langle\epsilon\rangle r$. Similarly there is also an exact scaling relation for the third order cross correlation given by Yaglom [22]: $\langle\Delta u_r(\Delta T_r)^2\rangle = -4/3\langle N\rangle r$. To demonstrate the quality of the inertial range scaling of our DNS data, in Fig. 1 we present $-\langle(\Delta u_r)^3\rangle/r\langle\epsilon\rangle$ and $-\langle\Delta u_r(\Delta T_r)^2\rangle/r\langle N\rangle$ as functions of r. It is seen that both quantities show a narrow inertial scaling range (less than one decade and they are also displaced with respect to each other). On the other hand, although DNS was carried out at moderate Reynolds numbers, the values of the dimensionless constants agree well with theoretical predictions (4/5 and 4/3 for velocity and passive scalar, respectively). It was reported in reference [23] that these dimensionless constants were smaller in the experimental measurements (for a circular jet with $\mathcal{R}_\lambda = 220$ and the atmospheric surface layer with $\mathcal{R}_\lambda = 7200$) than the theoretical values. In the inset, we show the passive scalar spectrum, $E_p(k)$, as a function of the wave number, k. The inertial range with a slope slightly less than $-5/3$ [7] could be identified. This smaller than $-5/3$ exponent was previously observed experimentally [24]. A bump between the inertial and dissipation ranges perhaps is associated with the "bottleneck effect" [25].

In Fig. 2, we plot structure functions, $\langle|\Delta T_r|^p\rangle$, as functions of r for $p = 2, 4, 6$ and 8. The power law inertial range can be identified for $0.2 \le r \le 1$. From data analysis we notice that in fact the passive scalar increment displays a better scaling relation than the velocity increment [19], and therefore it is not necessary to invoke the Extended-Self-Similarity (ESS) technique [26]. As a matter of fact we have tried ESS by plotting $\langle|\Delta T_r|^p\rangle$ as a function of $\langle\Delta u_r(\Delta T_r)^2\rangle$. The error bar for the extracted scaling exponents in the inertial range seems bigger than the result using the original structure functions. In inset (a), we show the local slope, $z_p(r) = d\log S_p(r)/d\log r$, as a function of r for the same p in the structure function. The local slope was calculated using a least square fit to a power law for every 3 neighboring points. A flat region for each p can be seen for $z_p(r)$, supporting the existence of inertial scaling range. In inset (b), we present the two point correlation function of the passive scalar dissipation function, $\langle N(x)N(x+r)\rangle$, as a function of r. Again a scaling relation for the dissipation correlation is found: $\langle N(x)N(x+r)\rangle \sim r^{-\mu}$ with $\mu \approx 0.25$. The intermittency parameter μ agrees well with previous experimental results [17].

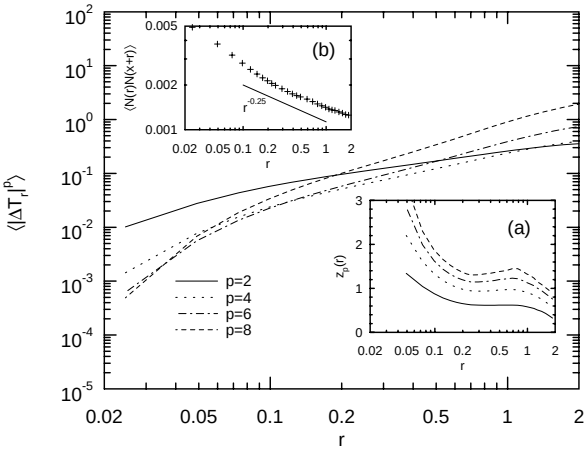

FIG. 2. The structure function $S_p(r)$ as a function of r. In the inset (a) shows the local slope $z_p(r)$ as a function of r and in the inset (b), we present the two-point correlation function of the passive scalar dissipation.

In Fig. 3, we show the normalized probability density function (PDF), $\langle D\rangle P(D)$, as a function of the normalized fluctuation dissipation: $D/\langle D\rangle$, where D is the dissipation function. It is clear that both the velocity dissipation and the scalar dissipation fields are strongly intermittent [27]. We have also compared the PDFs with the log-normal distribution by looking at the statistics of $w_D = (lnD - \langle lnD\rangle)/\langle(lnD - \langle lnD\rangle)^2\rangle^{1/2}$. It is found that both fields are quite close to the log-normal values for low order moments. From the plot, we also note that the PDF of the scalar dissipation has a wider tail than that of the velocity dissipation, indicating that spatially there are more large amplitude events in the passive scalar dissipation than the velocity dissipation. In the inset we show the flatness of the passive scalar increment and the longitudinal velocity increment as functions of the separation. It is seen that the flatness of the scalar increment is larger than that of the longitudinal velocity increment, except when r is in the large scale region

where both fields are essentially Gaussian and their flatnesses approach the Gaussian value of 3. In particular, when r is in the dissipation range, the flatness of the passive scalar increment is significantly larger than that of the velocity increment, in agreement with the PDFs.

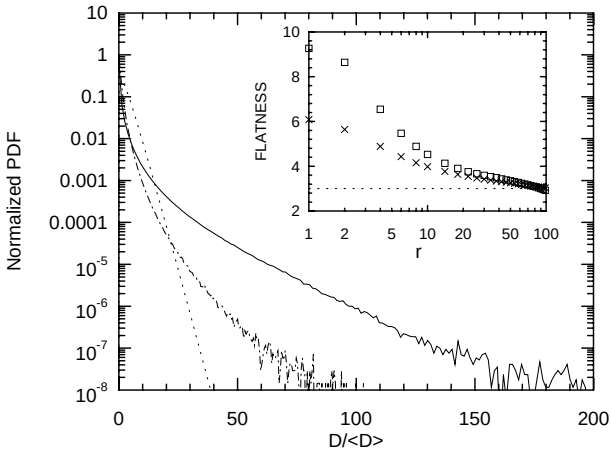

FIG. 3. Normalized PDF, $\langle D\rangle P(D)$ as a function of the normalized dissipation. Here D is the dissipation function (the solid line is for the scalar dissipation and the dotted-dash line for the velocity dissipation). The dotted line is for the scalar dissipation function with Gaussian statistics. In the inset we present the flatness of the scalar increment ($\Box$) and the velocity increment ($\times$) as a function of r (lattice unit).

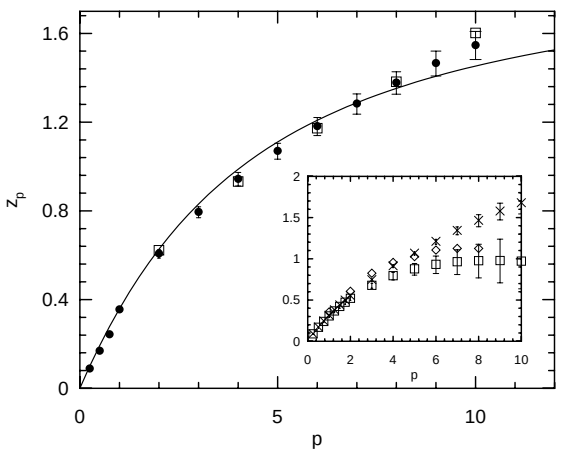

FIG. 4. The scaling exponent, z_p, as a function of p. The $\bullet$ sign is for DNS and the $\Box$ for the experiment data in [17]. The solid line is for a bi-variate log-Poisson model in [15]. In the inset shows the scaling exponents at two different time steps without using time averaging. The data from [14] are represented by the $\diamond$ sign.

The scaling exponent, z_p, as a function of the order index, p, is shown in Fig. 4. The $\bullet$ sign is for the result from DNS measurement and the $\Box$ sign for the result from the experiment by Antonia *et al.* [17]. The solid line is from a bi-variate log-Poisson model in [15] assuming that the correlation coefficient between velocity field and the passive scalar field is zero. The DNS scaling exponents are obtained using the flat region in the the local slope plot as shown in the inset (a) of Fig. 2. Some typical scaling exponents and the corresponding errors are listed here: $z_{0.5} = 0.165 \pm 0.007, z_1 = 0.354 \pm 0.012, z_2 = 0.606 \pm 0.019, z_3 = 0.794 \pm 0.025, z_4 = 0.943 \pm 0.030, z_6 = 1.180 \pm 0.041, z_8 = 1.376 \pm 0.050$ and $z_{10} = 1.546 \pm 0.063$. It is noticed that the second order scaling exponent deviates from Obukhov's 2/3 law by 15%. This result agrees well with previous experimental results [17,14,24]. The fourth order scaling exponent in DNS also agrees quite well with the theoretical prediction: $z_4 = 2z_2 - \mu$ in [4], a result primarily for the white and Gaussian velocity. In general, all scaling exponents from DNS coincide well with the phenomenological theory [15] and the real-life experiment [17].

We point out that the DNS results shown in Fig.4 were obtained using a spatial averaging over the whole simulation domain (512^3) and a long-time averaging ($\sim$ 10 large-eddy turnover times). In fact, the scaling exponent for each single time frame displays intense fluctuation with time, much larger than the fluctuation of the exponents for the velocity increment [19] using a spatial averaging of the same size. To demonstrate this fluctuation, in the inset of Fig. 4, two typical scaling exponents without time averaging are shown. The time difference between two frames is about 0.2 large-eddy turnover time. Although the curves for $p \leq 4$ agree quite well, they are qualitatively different for larger p. A large variation of the corresponding PDFs with time has also been observed. One set of the scaling exponents ($\Box$) clearly establishes a saturation when $p \geq 7$, indicating a possible upper bound for the most intensive events. The saturation of scaling exponents for the passive scalar has been observed in [14] (shown also in the inset by the $\diamond$ sign) and [28]. The scaling exponents in another group ($\times$) are larger than the time-averaged values in Fig. 4 for $p \geq 5$. Such strong fluctuations could be a reason for the saturation displayed in [14] where the results were obtained based on 1-D cuts through the field and may not capture the strongest events with a limited sample. On the other hand, the experimental scaling exponents were obtained through the RSH and it can not be ruled out that the saturation could be due to shortcomings of the RSH at high values of p.

To understand the physics behind the large time fluctuation of the scaling exponent, we have studied the intermittency structures of the passive scalar field, in particular the large amplitude events of the dissipation function and the scalar derivative. The latter is directly associated with the scalar increment: $\Delta T_r = \int_0^r \partial(T/\partial x)dx$. Using visualization technique, we find that with increasing of amplitude, the iso-surface of the scalar dissipation changes from fragment-like to sheet-like (shown in Fig. 5). The dynamical evolution of the sheet-like structures, such as formation and annihilation, clearly plays a key role in the time dependence of the scaling exponents, simply because the large amplitude events are the predomi-

nate effects on the high order scalar increments and their exponents. From the structure stability point of view, we suspect that the sheet-like structure are more unstable to perturbations, such as forcing, than the filament-like structure [30], which is a characteristic vortex structure for large amplitude events in three-D turbulence. This agrees with the observation that the velocity scaling exponent seems to be less time dependent. The instability of the sheet-like structures possibly causes the annihilation of the very high intermittency structures at a specific time, leading to a saturation of the scaling exponents. In addition, we know from Fig. 3 that spatially there are more high amplitude events in the scalar field than in the velocity field, indicating that the generation and the annihilation of the sheet-like structure is more frequent and causes intense fluctuations in the statistics of the scalar field.

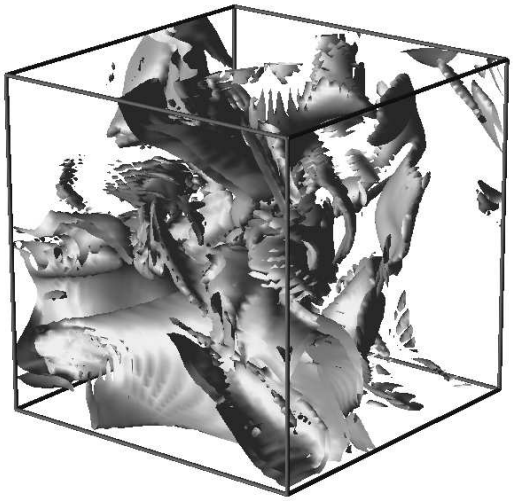

FIG. 5. Iso-surface of the scalar dissipation at the value $N = 10\langle N\rangle$. The resolution of the plot is 64^3 and the data shown represent the neighborhood of the overall maximum of scalar dissipation.

The current finding of the time dependence of the scaling exponents might connect with the idea of the non-universality of scaling exponents for the passive scalar system [29] in the sense that the detailed intermittency structure strongly affects the exponents. On the other hand, so far little is known about how the velocity stretching affects the dynamical evolution of the sheet-like structure in the scalar field. We feel that the fundamental physics of the scaling dynamics for the passive scalar turbulence is still missing and a more detailed and careful study is much needed.

We thank R. Kraichnan, C. Meneveau, M. Nelkin, Z.-S. She and K. R. Sreenivasan for useful discussions. Numerical simulation was carried out at the Advanced Computing Laboratory at Los Alamos National Laboratory.

[1] M. Avellaneda and A. Majda, Commun. Math. Phys. **131**, 381 (1990).
[2] R. H. Kraichnan, Phys. Rev. Lett. **72**, 1016 (1994)]
[3] V. S. L'vov, I. Procaccia, and A. L. Fairhall, Phys. Rev E, **50**, 4684 (1994); M. Chertkov, G. Falkovich, I. Kolokolov, and V. Lebedev, Phys. Rev. E, **52**, 4924 (1995); K. Gawcedzki and A. Kupiainen, Phys. Rev. Lett. **75**, 3608 (1995); G. L. Eyink, Phys. Rev. E, **54**, 1497 (1996).
[4] R. H. Kraichnan, V. Yakhot, and S. Chen, Phys. Rev. Lett. **7 5**, 240 (1995)
[5] E. S. C. Ching, V. S. L'vov, and I Procaccia, Phys. Rev. E, **54**, 6364 (1996).
[6] A. N. Kolmogorov, C. R. Acad. Sci. URSS **30** 301 (1941)
[7] A. M. Oboukov, Izv. Akad. Nauk. SSSR, Geor. i. Geofiz. **13**, 58 (1949).
[8] S. Corrsin, J. Appl. Phys. **22**, 469 (1951).
[9] A. Y. S. Kuo and S. Corrsin, J. Fluid Mech. **50** 285 (1971); P. Kailasnath, K. R. Sreenivasan, and G. Stolovitzky, Phys. Rev. Lett. **68**, 2766 (1992).
[10] A. N. Kolmogorov, J. Fluid Mech. **13**, 82 (1962).
[11] G. Stolovitzky, P. Kailasnath and K. R. Sreenivasan, J. Fluid Mech., **297**, 275 (1995);S. Chen, G. D. Doolen, R. H. Kraichnan and Z.-S. She, Phys. of Fluids A, **5**i, 458 (1993).
[12] C. W. Van Atta, Phys. Fluids **14**, 1803 (1971).
[13] U. Frisch, P-L. Sulem, and M. Nelkin, J. Fluid. Mech. **87**, 719 (1978).
[14] C. Meneveau, K. R. Sreenivasan, P. Kailasnath, and M. S. Fan, Phys. Rev. A **41**, 894 (1990).
[15] N. Cao and S. Chen, "An Intermittency Model For Passive-Scalar Turbulence," Phys. Fluids, (in press), 1997.
[16] K. R. Sreenivasan and R. A. Antonia, Annu. Rev. Fluid Mech. (in press), (1996).
[17] R. A. Antonia, E. J. Hopfinger, Y. Gahnei, and F. Anselmet, Phys. Rev. A **30**, 2704 (1984).
[18] G. Ruiz Chavarria, C. Baudet and S. Ciliberto, Europhys. Lett., **32**, 319, (1995).
[19] N. Cao, S. Chen and Z.-S. She, Phys. Rev. Lett., **76**, 3711 (1996).
[20] R. Kerr, J. Fluid Mech., **153**, 31 (1985).
[21] A. N. Kolmogorov, C. R. Acad. Sci. USSR **32**, 16 (1941).
[22] A, M, Yaglom, Dokl. Akad. Nauk. SSSR **69**, 743 (1949).
[23] Y. Zhu, R. A. Antonia, and I. Hosokawa, Phys. Fluids, **7**, 1637 (1995).
[24] Jayesh, C. Tong and Z. Warhaft, Phys. Fluids, **6**, 306 (1994).
[25] D. Lohse and A. Müller-Groeling, Phys. Rev. Lett. **74**, 1747 (1995); G. Falkovich, Phys. Fluids **6**, 1411 (1994).
[26] R. Benzi, S. Ciliberto, R. Tripiccione, C. Baudet, E. Massaioli and S. Succi, Phys. Rev. E. **48**, 29 (1993).
[27] K. R. Sreenivasan and R. A. Antonia, Phys Fluids, **20**, 1238 (1977).
[28] V. Borue, Private communication, (1996).
[29] B. Shraiman and E. Siggia, C. R. Acad. Sci. **321**, 279 (1995); Chertkov G. Falkovich and V. Lebedev, Phys. Rev. Lett. **76**, 3707 (1996)

[30] E. D. Siggia, J. Fluid Mech. **107**, 375 (1981); Z.-S. She, E. Jackson and S. A. Orszag, Nature, **344**, 226 (1990); J. Jimenez, A. A. Wray, P. G. Saffman and R. S. Rogallo, J. Fluid Mech. **255**, 65 (1993).